Quantitative Assessment of Coumarin-Containing Polymer Film's Capability for Photoalignment of Liquid Crystals

Chunki Kim,[†] Jason U. Wallace,[†] Anita Trajkovska,[†,‡] Jane J. Ou,[†] and Shaw H. Chen*[,†,§]

Department of Chemical Engineering and Laboratory for Laser Energetics, University of Rochester, 240 East River Road, Rochester, New York 14623

Received September 15, 2007; Revised Manuscript Received October 6, 2007

ABSTRACT: The photoalignment of a nematic fluid, E-7, and a glassy-nematic oligofluorene, **F(MB)5**, was investigated on films of **Polymers 1** and **2** in the parallel regime. Polarized absorption spectroscopy and computational chemistry were employed to characterize coumarin monomer's and dimer's molar extinction coefficients and to locate absorption dipoles as parallel to their long molecular axes. Moreover, their orientational order parameters, S_m and S_d, were experimentally determined as functions of the extent of dimerization. Higher S_d and Y_d, coumarin dimer's mole fraction, were achieved in films of **Polymer 1** than in **Polymer 2** because of the greater coumarin mobility of the former. The ability of a coumarin-containing photoalignment film to orient a spin-cast **F(MB)5** film was found to improve with increasing Y_dS_d to an extent comparable to that of a rubbed polyimide film. Because of the relatively short lengths of its constituent molecules, E-7 was oriented equally well on both polymer films regardless of the Y_dS_d values.

Introduction

Traditionally mechanical rubbing has been widely practiced for the preparation of electrooptic devices consisting of liquid crystals. As a noncontact alternative to rubbing, photoalignment has been actively pursued[1] in recent years to avoid the problems arising from rubbing, such as dust, electrostatic charges, and damage to alignment coatings. In addition, photoalignment is instrumental to the realization of wide viewing angles in liquid crystal displays[2,3] and modulation of diffraction gratings.[4−6] There are three distinct approaches to photoalignment induced by polarized irradiation: photodegradation of polyimides,[7−12] cis−trans isomerization of azobenzenes,[13−20] and (2 + 2) cycloaddition of cinnamates or coumarins.[21−39] It has been demonstrated that coumarins are advantageous in thermal and photochemical stability, absence of photoinduced isomerization, and accessibility to a wide range of pretilt angle. In principle, photoalignment is accomplished on a coumarin-containing polymer film that has been treated with linearly polarized UV-irradiation (i.e., 300−350 nm) to define an axis along which monomers are preferentially dimerized. As dimerization proceeds, the increasingly populated dimers become less ordered along the polarization axis, while the diminishing monomers become better oriented in the perpendicular direction. In this process, coumarin dimers and monomers compete for liquid crystal orientation, resulting in crossover from a parallel to a perpendicular alignment at an intermediate extent of dimerization.[31,32,38,39]

With the assumption of no orientational relaxation involving coumarin dimers or monomers, we have constructed a kinetic model for the prediction of the orientational order parameters governing coumarin dimers and monomers as functions of the extent of dimerization.[38] Three parameters are relevant to liquid crystal orientation including the crossover behavior: relative abundance and orientation order of coumarin dimers and monomers in addition to the energetics of their interactions with liquid crystalline molecules. On the basis of this kinetic model, we have also demonstrated that it is the interplay between these three parameters, as opposed to photodegradation, that is responsible for crossover in liquid crystal orientation.[32,39] The present study aims to devise a methodology for the experimental determination of coumarin dimers' and monomers' orientational order parameters at the early stage of polarized UV-irradiation, where dimers are responsible for aligning liquid crystals. The product of dimers' concentration and orientational order parameter will serve to quantitatively assess the photoalignment film's ability to orient liquid crystals.

Experimental Section

Materials Synthesis. The reaction schemes as well as the synthesis and purification procedures for **Polymer 2** are included in the Supporting Information. The analytical and ^{1}H NMR spectral data are presented in what follows.

Poly[7-[[4-[[[3-(methacryloyl)oxy]propyl]oxy]benzoyl]oxy]-coumarin], Polymer 2. Anal. Calcd: C, 67.64; H, 4.94. Found: C, 67.31; H, 4.84. ^{1}H NMR spectral data (400 MHz, $CDCl_3$): δ (ppm) 0.85−1.82 (5H, polymer main chain), 2.09 (2H, $-CH_2CH_2-CH_2-$) 4.05 (4H, $-COOCH_2-$, $-CH_2OAr-$), 6.30 (1H, $-HC{=}CHCO-$, coumarin), 6.93 (2H, aromatics), 7.09 (2H, coumarin), 7.45 (1H, coumarin), 7.63 (1H, $-HC{=}CHCO-$, coumarin), 8.05 (2H, aromatics).

Phase Transition Temperatures and Polymer Molecular Weights. Thermal transition temperatures of **Polymers 1** and **2** and **Copolymer** were determined by differential scanning calorimetry, DSC (Perkin-Elmer DSC-7), with a continuous N_2 purge at 20 mL/min. Samples were preheated up to 200 °C followed by cooling to −30 °C before taking the reported heating and cooling scans at 20 °C/min. The nature of phase transitions was characterized with a polarizing optical microscope (DMLM, Leica, FP90 central processor) coupled with a hot stage (FP82, Mettler Toledo). Polymer molecular weights were characterized in *N*-methylpyrrolidone containing 0.02 M lithium bromide at 60 °C using size-exclusion chromatography (model 301 TDA, Viscotek) based on universal calibration involving polystyrene standards (Pressure Chemical Company).

* Author to whom all correspondence should be addressed.
[†] Department of Chemical Engineering, University of Rochester.
[‡] Present address: Bright View Technologies, 5151 McCrimmon Parkway, Morrisville, NC 27560.
[§] Laboratory for Laser Energetics, University of Rochester.

10.1021/ma702080z CCC: $37.00
Published on Web 11/15/2007

Chart 1. Polymers 1 and 2, Copolymer, and F(MB)5 Used under Present Investigation

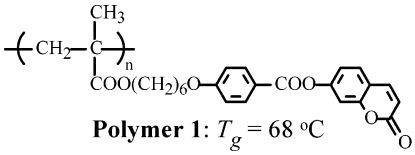

Polymer 1: T_g = 68 °C

$\overline{M}_w$ = 76,300 g/mole; $\overline{M}_w/\overline{M}_n$ = 3.3

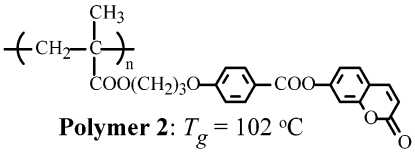

Polymer 2: T_g = 102 °C

$\overline{M}_w$ = 58,000 g/mole; $\overline{M}_w/\overline{M}_n$ = 3.4

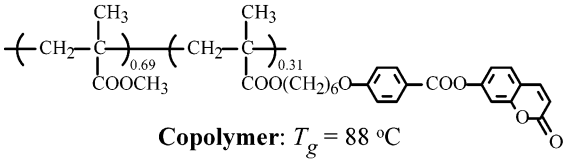

Copolymer: T_g = 88 °C

$\overline{M}_w$ = 48,700 g/mole; $\overline{M}_w/\overline{M}_n$ = 2.1

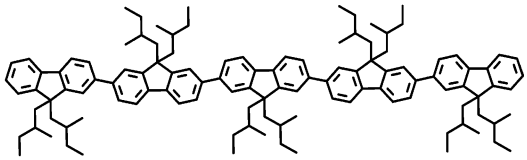

F(MB)5: T_g = 89 °C, T_c = 167 °C

Determination of Monomer's and *syn-hh* Dimer's Absorption Dipoles. To locate the absorption dipoles of **Monomer** at 264 and 310 nm and of ***syn-hh*** **Dimer** at 264 nm, 10-μm-thick sandwiched cells were prepared with the fused silica substrates coated with uniaxially rubbed Nylon-66. A UV-transparent nematic liquid crystal, ZLI-2359 (Merck), containing **Monomer** at 3.0 wt % and ***syn-hh*** **Dimer** at 0.25 wt % was injected into the cell gap in the isotropic state (at 80 °C) to avoid flow-induced alignment. After annealing at 60 °C for 0.5 h, the cells were cooled at 10 °C/h to room temperature. Absorption dichroism was measured with a UV−vis-NIR spectrophotometer (Lambda-900, Perkin-Elmer) equipped with a Glan−Thompson polarizer (Newport).

Preparation and Characterization of Photoalignment Films. For the alignment of the nematic liquid crystal and the monodisperse glassy-nematic oligofluorene, films of **Polymers 1** and **2** were prepared by spin-casting at 4000 rpm from 0.1 wt % chloroform solutions on optically flat fused silica substrates transparent to 200 nm (Esco Products). Polymer films were spin-cast at 5000 rpm from 1.0 wt % chloroform solutions on the same fused silica substrates for characterizations with variable angle spectroscopic ellipsometry (V-VASE, J. A. Woollam Corporation) and UV−vis−NIR absorption spectrophotometry. Irradiation of films of **Polymers 1** and **2** was performed at 120 and 160 °C, respectively, under argon with a 500 W Hg−Xe lamp (model 66142, Oriel) equipped with a filter (model 87031, Oriel) that cuts off wavelengths below 300 nm and a dichroic mirror that reflects light between 260 and 320 nm (model 66217, Oriel). Linearly polarized irradiation was achieved using a polarizing beam splitter (HPB-308 nm, Lambda Research Optics, Inc). The irradiation intensity was monitored by a UVX digital radiometer coupled with a UVX-31 sensor (UVP, Inc.). The extent of dimerization was characterized by monitoring the UV−vis absorbance of coumarin monomers at 310 nm where dimers are transparent. The polarized UV−vis absorption was measured using a spectrophotometer equipped with a Glan−Thompson polarizer to determine the orientational order parameter of the monomers and dimers in the irradiated films. Insolubility of irradiated films was determined by UV−vis absorption spectroscopy after rinsing with chloroform.

Photoalignment of a Nematic Liquid Crystal and Glassy-Nematic Oligofluorene. For the characterization of their ability to orient a nematic liquid crystal, irradiated films of **Polymers 1** and **2** on fused silica substrates were used to prepare 10-μm-thick sandwiched cells. A commercially available nematic liquid crystal, E-7 (Merck), containing a dichroic dye, M-137 (Mitsui Toatsu Dyes, Ltd.), at 0.3 wt % was injected into the cell gap in the isotropic state (at 65 °C) to avoid flow-induced alignment. After annealing at 50 °C for 0.5 h, the cells were cooled at 10 °C/h to room temperature. A spectrophotometer equipped with a linear polarizer (HNP′B, Polaroid) was used to measure the orientational order parameter. Fresnel reflections from the air−glass interfaces were accounted for using a reference cell comprising an index-matching fluid sandwiched between two alignment-treated substrates. The ability of **Polymers 1** and **2** films to orient glassy-nematic **F(MB)5** was also appraised. Approximately 50-nm-thick films were spin-cast from 0.5 wt % chloroform solutions on fused silica substrates coated with photoalignment films. After vacuum-drying overnight, **F(MB)5** films were annealed above their glass transition temperature under argon for 0.5 h. Polarized UV−vis absorption spectroscopy was employed to determine the orientational order parameter.

Results and Discussion

Two coumarin-containing polymers were used in this study to evaluate their ability to orient a commercially available nematic liquid crystal, E-7, and a glassy-nematic pentafluorene, **F(MB)5**.[40] The molar extinction coefficients of the coumarin monomer were characterized using binary mixtures of **Copolymer** with **Polymer 1** and poly(methylmethacrylate), PMMA, to ensure miscibility. The structures of **Polymers 1** and **2**, **Copolymer**, and **F(MB)5** are depicted in Chart 1 together with their glass transition temperatures (T_g), clearing temperatures (T_c), weight-average molecular weights ($\bar{M}_w$), and polydispersity factors ($\bar{M}_w/\bar{M}_n$) with $\bar{M}_n$ representing the number-average molecular weight.

Fused silica substrates coated with polarized UV-irradiated, 10-nm-thick **Polymers 1** and **2** films were used to prepare sandwiched cells containing E-7 lightly doped with a dichroic dye, M-137, and spin-cast **F(MB)5** films for the characterization of respective orientational order parameters, S_{lc} and S_{OF}. Presented in Table 1 are the observed S_{lc} and S_{OF} values as functions of X, the extent of coumarin dimerization characterized by a previously reported procedure.[38,39] It is evident that a consistently higher X was achieved with **Polymer 1** than **Polymer 2** at the same fluence level. Apparently, at the same

Table 1. Extent of Dimerization, *X*, Orientational Order Parameter of E-7 Doped with M-137, S_{lc}, That of F(MB)5, S_{OF}, and the Product of Coumarin Dimers' Mole Fraction and Orientation Order Parameter, Y_dS_d, as Functions of Fluence

	Polymer 1[a]				Polymer 2[b]			
fluence, J/cm^2	X	S_{lc}[c]	S_{OF}[d]	$100Y_dS_d$[e]	X	S_{lc}[c]	S_{OF}[d]	$100Y_dS_d$[e]
0.2	0.23	∥0.73	∥0.72	0.39	0.17	∥0.75	∥0.14	0.21
0.5	0.34	∥0.75	∥0.73	0.41	0.27	∥0.75	∥0.10	0.25
1.0	0.44	∥0.71	∥0.68	0.40	0.37	∥0.75	∥0.08	0.26
2.0	0.55	∥0.75	∥0.36	0.34	0.49	∥0.76	∥0.03	0.21

[a] Insolubility of 10-nm-thick film achieved at 0.2 J/cm^2 at an irradiation temperature of 120 °C. [b] Insolubility of 10-nm-thick film achieved at 0.2 J/cm^2 at an irradiation temperature of 160 °C. [c] 10-μm-thick nematic cells of E-7 doped with M-137. [d] 50-nm-thick spin-cast **F(MB)5** films annealed at 130 °C under argon for 30 min. [e] $Y_d = X/2$. S_{lc} and S_{OF} accompanied by an uncertainty of ±0.02 and 0.03, respectively.

Chart 2. Molecular Structures of Monomer and *syn-hh* Dimer and Their Energy-Minimized Geometries with Absorption Dipoles Identified as Double Arrows by Computational Chemistry Using Gaussian 03 Software Package

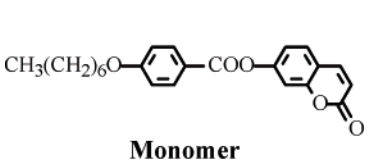

Monomer

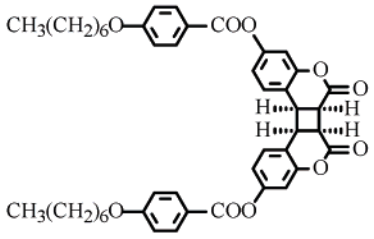

***syn-hh* Dimer**

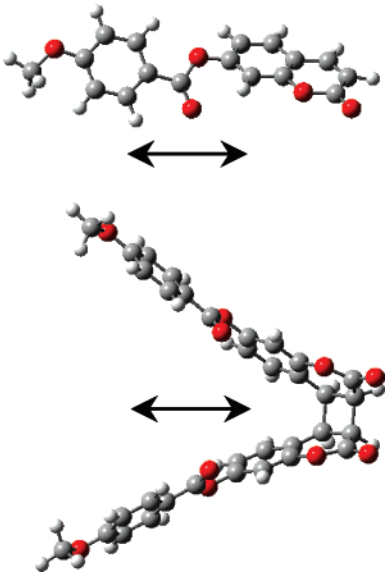

reduced irradiation temperature, $T_{irr}/T_g = 1.15$, the longer spacer in **Polymer 1** than in **Polymer 2** facilitated rotational diffusion of pendant coumarin monomers into the polarization axis for photodimerization. It is encouraging that all S_{lc} and some S_{OF} values are comparable to those achieved on conventional rubbed polyimide films.[38−40] The S_{OF} values on **Polymer 2**, however, were barely observable, which will be further investigated in what follows.

In a recent paper,[38] we have constructed a framework for describing photoalignment of liquid crystals in terms of the relative abundance of coumarin monomers and dimers, their respective orientational order, and the energetics of their interaction with overlying liquid crystals. As shown in Table 1, a parallel orientation of both E-7 and **F(MB)5** persisted up to a fluence of 2.0 J/cm^2, where coumarin dimers are responsible for photoalignment. In this regime, the photoalignment behavior is dictated by the coumarin dimers' concentration and orientational order parameter. The coumarin dimers' concentration in a UV-irradiated polymer film is directly proportional to X. For the characterization of the dimers' orientational order parameter, S_d, previously reported **Monomer** and ***syn-hh* Dimer**[39] depicted in Chart 2 were used to determine feasible absorption spectral ranges and to locate UV−vis absorption dipoles. Also included in Chart 2 are **Monomer**'s and ***syn-hh* Dimer**'s energy-minimized geometries, with methoxy instead of heptyloxy tails to facilitate computation, using B3LYP functionals with the 6-31G(d) basis set as part of the Gaussian 03 software package. The simplified structures are not expected to alter the computed geometries or absorption dipoles of 7-(benzoyloxy)coumarin before and after dimerization.

The normalized absorption spectra of **Monomer** and ***syn-hh* Dimer** doped in PMMA at a mole fraction $Y = 0.050$, on the basis of methacrylate monomer, are shown in Figure 1. The absorption maximum at 310 nm is attributable to **Monomer**'s 7-coumarin moiety, while that at 277 nm is contributed to mostly by the 4-heptyloxy benzoate moiety as Figure 1 here is compared to Figure 1a in ref 38. Upon dimerization, these two moieties in ***syn-hh* Dimer** have largely overlapping absorption maxima, resulting in a single peak at 264 nm. Computational chemistry also yielded **Monomer**'s and ***syn-hh* Dimer**'s absorption dipoles parallel to their long molecular axes, indicated as double arrows in Chart 2, for the absorption peaks shown in Figure 1.

To validate the absorption dipoles prescribed by computational chemistry, **Monomer** and ***syn-hh* Dimer** were lightly doped in a UV-transparent nematic liquid crystal, ZLI-2359, for the preparation of 10-μm-thick cells using fused silica substrates coated with uniaxially rubbed Nylon-66 films. Nylon-66 was used in place of polyimide to ensure transparency to the **Monomer**'s absorption range. The polarized absorbance profiles shown in Figure 2 reveal that **Monomer**'s absorption dipoles at 264 and 310 nm and that of ***syn-hh* Dimer**'s at 264 nm are all aligned with the rubbing direction that defines both the host and guest molecules' long molecular axes. These experimental observations support the computational results displayed in Chart 2, thereby inspiring confidence in compu-

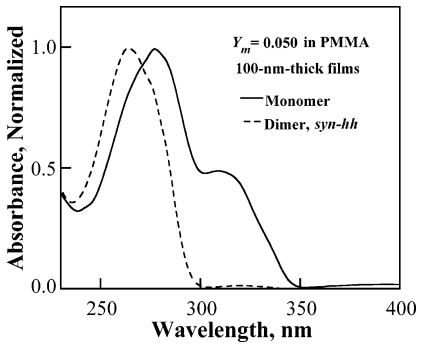

Figure 1. Normalized UV−vis absorption spectra of approximately 100-nm-thick films of **Monomer** and ***syn-hh* Dimer** doped in PMMA films at $Y_m = 0.050$.

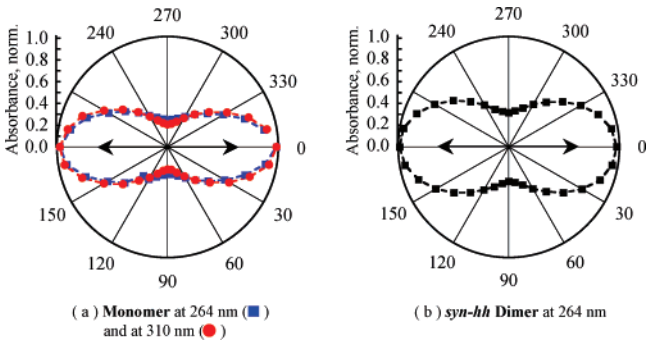

Figure 2. Polarized absorption profiles of 10-μm-thick cells comprising (a) **Monomer** at 3.0 wt % and (b) ***syn-hh* Dimer** at 0.25 wt % in ZLI-2359 between Nylon-66 films rubbed along double arrows.

Chart 3. Molecular Structures of *anti-hh, syn-ht, anti-hh* Dimers and Their Energy-Minimized Geometries with Absorption Dipoles Identified as Double Arrows by Computational Chemistry Using Gaussian 03 Software Package

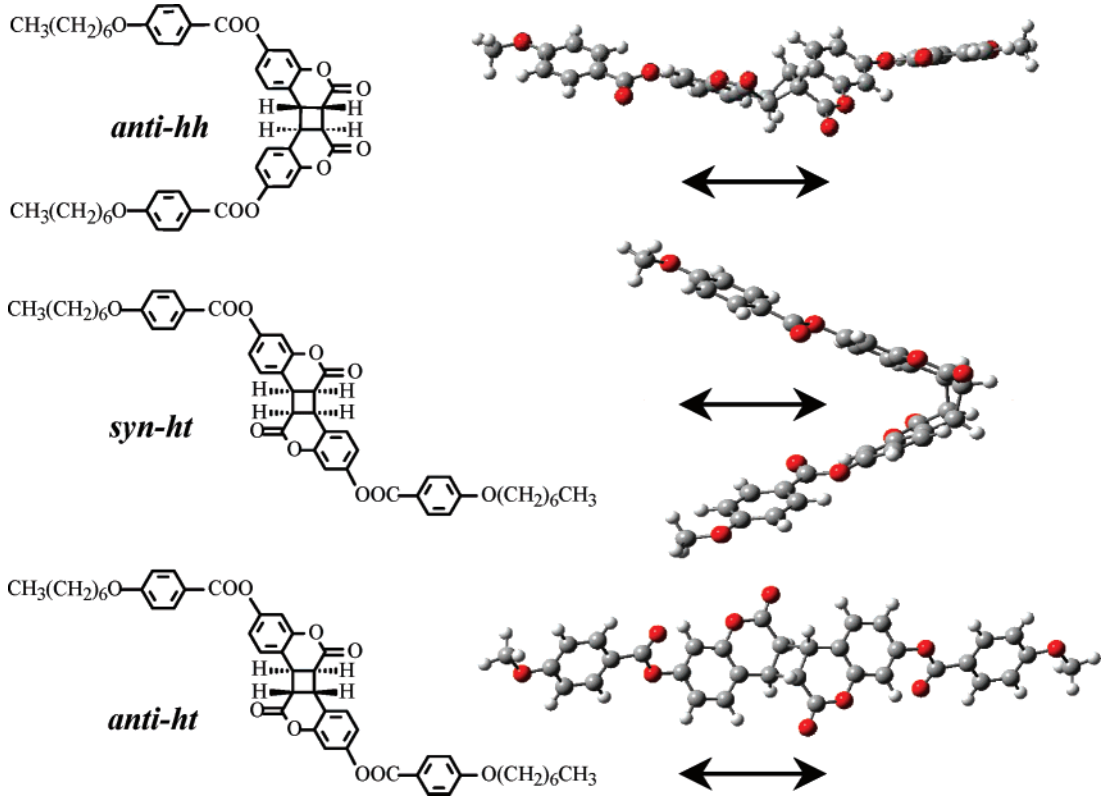

tational chemistry for representing molecular geometries and absorption dipoles.

Computations were further performed for experimentally inaccessible ***anti-hh***, ***syn-ht***, and ***anti-ht*** isomers in preparation for a subsequent interpretation of polarized absorption spectra of UV-irradiated films of **Polymer 1**, for which the regioisomerism of the emerging coumarin dimers could not be experimentally characterized upon isolation or in situ. In all four regioisomers, the dimerized 7-(benzoyloxy)coumarin moieties are responsible for the UV−vis absorption above 250 nm. Moreover, the absorption spectra of 6-methyl coumarin dimers were shown to be unaffected by regioisomerism, ***anti-hh*** versus ***syn-hh***.[41] Therefore, it is reasonable to expect that the absorption spectrum of ***syn-hh*** **Dimer** reproduced in Figure 1 is applicable to the other three isomers. The computational results presented in Charts 2 and 3 indicate that transition dipoles at the absorption maxima in the neighborhood of 265 nm follow the apparent long molecular axes for all four regiosiomers.

In addition to **Monomer**'s and ***syn-hh*** **Dimer**'s absorption dipoles, their molar extinction coefficients (ϵ_m and ϵ_d) are required for the calculation of S_d. Phase separation was encountered in an attempt to dope **Monomer** in PMMA to a relatively high level as needed. To circumvent this problem, **Copolymer** shown in Chart 1 was used for the preparation of a series of binary mixtures with **Polymer 1** and PMMA to cover the full range of Y_m from 0.00 to 0.50. The absorption spectra compiled in Figure 4 of ref 39 were employed to calculate ϵ_m at 264 and 310 nm using the relationship $\alpha_m = 2.303\epsilon_m Y_m$ as established in Figure 3.

Pristine **Polymers 1** and **2** films are represented by an initial concentration, $Y_{mo} = {}^1/_2$. At any stage of photodimerization, $Y_m = (1 - X)/2$ and $Y_d = X/2$. Figure 4a presents the evolution of absorption spectra at an increasing fluence level. No photodegradation was encountered with **Polymer 1** or **2**, as illustrated in Figure 4a for **Polymer 1** by the presence of an isobestic point at 267 nm throughout the UV-irradiation process. Both coumarin monomers and dimers absorb light at 264 nm, where ϵ_d can be evaluated with the assumption that absorbances by the two moieties are additive. Thus, pendant monomers' contribution, $\epsilon_m Y_m L$, was subtracted from the total absorbance at 264 nm to arrive at α_d for the calculation of ϵ_d from the slope of the linear plot shown in Figure 4b.

Let us proceed to experimentally locate the coumarin dimer's absorption dipole at 264 nm relative to its long molecular axis using polarized absorption spectroscopy. A 78-nm-thick film of **Polymer 1** was irradiated with polarized UV to a fluence level of 0.2 J/cm^2 at 120 °C. Photodimerization in **Polymers 1** and **2** films may result in any or all of four possible regioisomers, but emerging dimers' absorption spectra above 250 nm are unaffected by regioisomerism, as noted above in relation to **Dimer**. Moreover, the transition dipoles associated with the absorption peaks around 265 nm are all parallel to the long molecular axes of the four regioisomers (see Charts 2 and 3). Polarized absorption spectra were collected for $A^{\parallel}$ and $A^{\perp}$ in

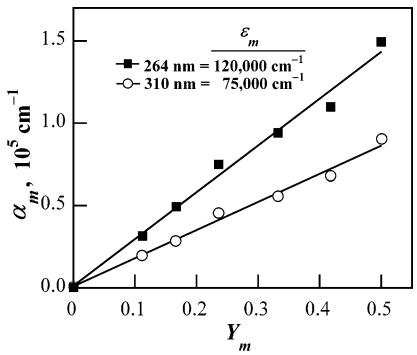

Figure 3. Direct proportionality of α_m to Y_m for the determination of ϵ_m at 264 and 310 nm.

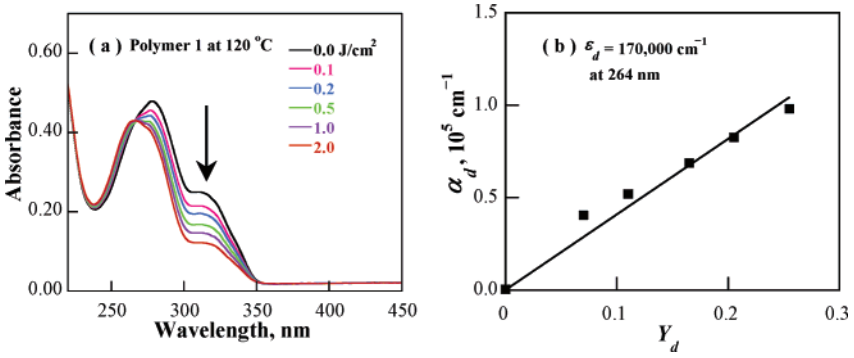

Figure 4. (a) UV−vis absorption spectra of 10-nm-thick **Polymer 1** films exposed to linearly polarized UV-irradiation at 120 °C to an increasing fluence as indicated by the arrow and (b) direct proportionality between α_d and Y_d for the determination of ϵ_d at 264 nm.

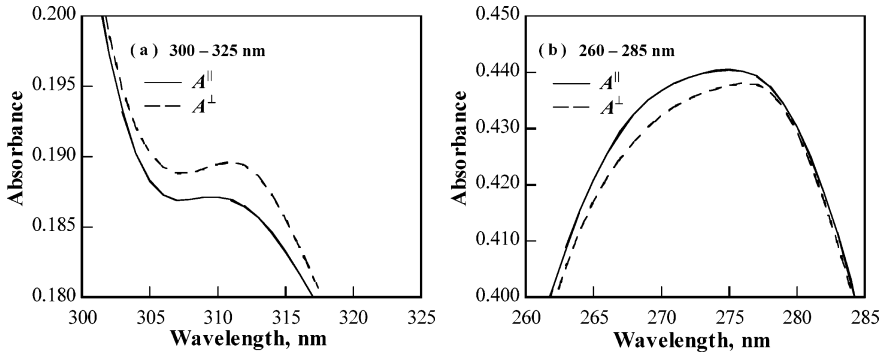

Figure 5. Polarized absorption spectra for (a) 300−325 nm and (b) 260−285 nm ranges of a 78-nm-thick **Polymer 1** film irradiated to a fluence level of 0.2 J/cm² at 120 °C; directions indicated by the superscripts on absorbance *A*, ∥ and ⊥, refer to the polarization axis of UV-irradiation.

Figure 5, in which superscripts ∥ and ⊥ represent the directions parallel and perpendicular to the polarization axis of UV-irradiation, respectively. As revealed in Figure 2a, coumarin monomer's absorption dipole at 310 nm lies along its long molecular axis. Under polarized irradiation across 300−320 nm, coumarin monomers with their absorption dipoles largely parallel to the polarization axis are preferentially consumed. Since coumarin dimers are transparent across 300−320 nm, one would expect $A^{\parallel} < A^{\perp}$, which is observed in Figure 5a. The coumarin monomer's absorption dipole at 264 nm also lies parallel to its long molecular axis according to Figure 2a. Therefore, the preferential depletion of coumarin monomers along the polarization axis would have resulted in $A^{\parallel} < A^{\perp}$ at 264 nm without considering the dimers' contribution to absorption dichroism of the irradiated film. The fact that $A^{\parallel} > A^{\perp}$ at 264 nm, as shown in Figure 5b, leads one to conclude that despite the unknown regioisomerism in the UV-irradiated **Polymer 1** film, the coumarin dimers' absorption dipoles must be largely parallel to their long molecular axes. This experimental observation validates the absorption dipoles predicted by computational chemistry for the four regioisomers of **Dimer** as shown in Charts 2 and 3.

While **Polymer 1** served to characterize molar extinction coefficients and absorption dipoles for coumarin monomers and dimers, the results are applicable to **Polymer 2** as well. With the coumarin monomer's and dimer's absorption dipoles lying parallel to their long molecular axes, both S_m and S_d can be calculated according to $S = (R - 1)/(R + 2)$, in which the absorption dichroic ratio $R = A^{\parallel}/A^{\perp}$. For the calculation of S_m, the polarized absorption spectra, such as Figure 5a, were used to determine $A^{\parallel}_m$ and $A^{\perp}_m$ for coumarin monomers at 310 nm. For the determination of S_d at 264 nm, monomers' contributions were subtracted from the total polarized absorbances to arrive at dimers' contributions as follows: $A^{\parallel}_{d,264} = A^{\parallel}_{t,264} - (\epsilon_{m,264}/\epsilon_{m,310})A^{\parallel}_{m,310}$ and $A^{\perp}_{d,264} = A^{\perp}_{t,264} - (\epsilon_{m,264}/\epsilon_{m,310})A^{\perp}_{m,310}$, in which

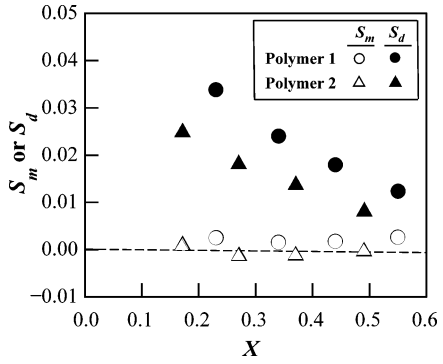

Figure 6. Experimentally characterized orientational order parameters for pendant coumarin monomers and dimers, S_m and S_d, in **Polymers 1** and **2** as functions of the extent of dimerization, *X*, effected by linearly polarized UV-irradiation at 120 and 160 °C, respectively.

subscripts d and t denote dimers' contribution and total absorbance, respectively, and 264 and 310 specify the wavelengths to which the absorbance and molar extinction coefficient are referred.

The results are presented in Figure 6 for S_m and S_d as functions of *X* with an objective of explaining why **Polymer 1** is superior to **Polymer 2** in the ability to orient **F(MB)5**. At the same reduced irradiation temperature, $T_{irr}/T_g = 1.15$, the pendant coumarin monomers in **Polymer 1** are more mobile than those in **Polymer 2** because of the longer flexible spacer. Pendant mobility of coumarin monomers is conducive to photodimerization as a result of rotational diffusion on the part of coumarin monomers into the polarization axis of UV-irradiation. Indeed, a higher extent of dimerization was achieved in **Polymer 1** than **2** at the same fluence (see Table 1). In addition, note the higher S_d values observed for **Polymer 1** than for **Polymer 2** as shown in Figure 6. It appears that once formed preferentially along the polarization axis, coumarin dimers are not as susceptible to thermal relaxation due in part to the dimers'

size doubling the monomers' and in part to dimers being anchored between two neighboring methacrylate polymer chains. In the absence of thermal relaxation, residual coumarin monomers are expected to become increasingly organized perpendicular to the polarization axis as photodimerization proceeds, resulting in an increasingly negative S_m value[38] that approaches -0.5 in the limit of complete dimerization. Thermal relaxation, however, appears to have diminished its absolute values to such an extent that $|S_m| \cong 0$ within an experimental error of ± 0.003 in all cases (see Figure 6). It is logical to appraise a coumarin-containing polymer film's capability for photoalignment in terms of Y_d and S_d. As **Polymer 1** is compared to **2**, the consistently higher Y_dS_d value appears to be responsible for the better orientational order of **F(MB)5** (see Table 1). In contrast, **Polymers 1** and **2** perform comparably well in their ability to align E-7 presumably because of the relatively short lengths of constituent molecules. In other words, the alignment of the longer **F(MB)5** molecules demands more concentrated coumarin dimers oriented to a higher degree than the shorter molecules comprising E-7.

Conclusions

Photoalignment of E-7 and **F(MB)5** was investigated on films of coumarin-based **Polymers 1** and **2** in the parallel regime, *viz.* prior to crossover in liquid crystal orientation. The ability to align liquid crystals was elucidated in terms of the coumarin dimers' concentration and orientational order parameter. Major accomplishments are recapitulated as follows: (1) Through polarized absorption spectroscopy and computational chemistry, the absorption dipoles of coumarin monomer and dimer were located as parallel to their long molecular axes. In addition, S_m and S_d were characterized as functions of X by absorption dichroism. (2) The higher X and S_d values in **Polymer 1** than in **Polymer 2** at the same fluence level and irradiation temperature relative to T_g originated from (i) the higher mobility of pendant coumarin monomers with a longer flexible length and (ii) the lack of mobility of pendant coumarin dimers in both polymers because of their size and anchoring between polymer chains. (3) As reflected by the S_{OF} values on **Polymer 1** compared to **2**, the photoalignment film's ability to orient **F(MB)5** is quantifiable by Y_dS_d because of the demand on coumarin dimers' concentration and orientational order. In contrast, the S_{lc} values indicate that E-7 is well aligned on both **Polymers 1** and **2** regardless of the Y_dS_d values because of the relatively short lengths of its constituent molecules.

Acknowledgment. The authors thank Stephen D. Jacobs and Kenneth L. Marshall of the Laboratory for Laser Energetics, LLE, at University of Rochester for helpful discussions and technical advice. They are grateful for the financial support provided by the Eastman Kodak Company, the New York State Center for Electronic Imaging Systems, and the National Science Foundation under Grant CTS-0204827. Jason U. Wallace acknowledges the support of a Horton Graduate Fellowship administered by the LLE. Additional funding was provided by the Department of Energy Office of Inertial Confinement Fusion under Cooperative Agreement No. DE-FC52-92SF19460 with LLE and the New York State Energy Research and Development Authority. The support of DOE does not constitute an endorsement by DOE of the views expressed in this article.

Supporting Information Available: Procedures for the synthesis and purification as well as analytical and PMR spectral data for **Polymer 2**. This material is available free of charge via the Internet at http://pubs.acs.org.

References and Notes

(1) O'Neill, M.; Kelly, S. M. *J. Phys. D: Appl. Phys.* **2000**, *33*, R67−R84.
(2) Schadt, M.; Seiberle, H.; Schuster, A. *Nature (London)* **1996**, *381*, 212−215.
(3) Schadt, M.; Seiberle, H. *J. Soc. Inf. Display* **1997**, *5*, 367−370.
(4) Gupta, V. K.; Abbott, N. L. *Science* **1997**, *276*, 1533−1536.
(5) Patel, J. J.; Rastani, K. *Opt. Lett.* **1991**, *16*, 532−534.
(6) Chen, J.; Bos, P. J.; Vithana, H.; Johnson, D. L. *Appl. Phys. Lett.* **1995**, *67*, 2588−2590.
(7) Hasegawa, M.; Taira, Y. *J. Photopolym. Sci. Technol.* **1995**, *8*, 241−248.
(8) Gong, S.; Kanicki, J.; Ma, L.; Zhong, J. Z. Z. *Jpn. J. Appl. Phys.* **1999**, *38*, 5996−6004.
(9) Lu, J.; Deshpande, S. V.; Gulari, E.; Kanicki, J.; Warren, W. L. *J. Appl. Phys.* **1996**, *80*, 5028−5034.
(10) Sung, S.-J.; Lee, J.-W.; Kim, H.-T.; Park, J.-K. *Liq. Cryst.* **2002**, *29*, 243−250.
(11) Xu, C.; Shiono, T.; Ikeda, T.; Wang, Y.; Takeuchi, Y. *J. Mater. Chem.* **2003**, *13*, 669−671.
(12) Zhong, Z.-X.; Li, X.; Lee, S. H.; Lee, M.-H. *Appl. Phys. Lett.* **2004**, *85*, 2520−2522.
(13) Gibbons, W. M.; Shannon, P. J.; Sun, S.-T.; Swetlin, B. J. *Nature (London)* **1991**, *351*, 49−50.
(14) Shannon, P. J.; Gibbons, W. M.; Sun, S.-T. *Nature (London)* **1994**, *368*, 532−533.
(15) Ichimura, K.; Suzuki, Y.; Seki, T.; Hosoki, A.; Aoki, K. *Langmuir* **1988**, *4*, 1214−1216.
(16) Ichimura, K. *Chem. Rev.* **2000**, *100*, 1847−1874.
(17) Ikeda, T. *J. Mater. Chem.* **2003**, *13*, 2037−2057.
(18) Furumi, S.; Kidowaki, M.; Ogawa, M.; Nishimura, Y.; Ichimura, K. *J. Phys. Chem. B* **2005**, *109*, 9245−9254.
(19) Sévigny, S.; Bouchard, L.; Montallebi, S.; Zhao, Y. *Liq. Cryst.* **2005**, *32*, 599−607.
(20) Kwok, H. S.; Chigrinov, V. G.; Takada, H.; Takatsu, H. *J. Display Technol.* **2005**, *1*, 41−50.
(21) Schadt, M.; Schmitt, K.; Kozinkov, V.; Chirgrinov, V. *Jpn. J. Appl. Phys.* **1992**, *31*, 2155−2164.
(22) Schadt, M.; Seiberle, H.; Schuster, A.; Kelly, S. M. *Jpn. J. Appl. Phys.* **1995**, *34*, L764−L767.
(23) Cull, B.; Shi, Y.; Kumar, S.; Schadt, M. *Phys. Rev. E* **1996**, *53*, 3777−3781.
(24) Obi, M.; Morino, S.; Ichimura, K. *Jpn. J. Appl. Phys.* **1999**, *38*, L145−L147.
(25) Kawatsuki, N.; Ono, H.; Takatsuka, H.; Yamamoto, T.; Sangen, O. *Macromolecules* **1997**, *30*, 6680−6682.
(26) Kawatsuki, N.; Matsuyoshi, K.; Hayashi, M.; Takatsuka, H.; Yamamoto, T. *Chem. Mater.* **2000**, *12*, 1549−1555.
(27) Kawatsuki, N.; Takatsuka, H.; Yamamoto, T. Ono, H. *Jpn. J. Appl. Phys.* **1997**, *36*, 6464−6469.
(28) Ichimura, K.; Akita, Y.; Akiyama, H.; Kudo, K.; Hayashi, Y. *Macromolecules* **1997**, *30*, 903−911.
(29) Stump, A.; Gubler, U.; Bosshard, C. *Opt. Lett.* **2005**, *30*, 1333−1335.
(30) Perny, S.; Barny, P. L.; Delaire, J.; Buffeteau, T.; Soursseau, C.; Dozov, I.; Forget, S.; Martinot-Lagarde, P. *Liq. Cryst.* **2000**, *27*, 329−340.
(31) Obi, M.; Morino, S.; Ichimura, K. *Chem. Mater.* **1999**, *11*, 656−664.
(32) Jackson, P. O.; O'Neill, M.; Duffy, W. L.; Hindmarsh, P.; Kelly, S. M.; Owen, G. J. *Chem. Mater.* **2001**, *13*, 694−703.
(33) Kawatsuki, N.; Goto, K.; Yamamoto, T. *Liq. Cryst.* **2001**, *28*, 1171−1176.
(34) Contoret, A. E. A.; Farrar, S. R.; Jackson, P. O.; Khan, S. M.; May, L.; O'Neill, M.; Nicholls, J. E.; Kelly, S. M.; Richards, G. J. *Adv. Mater.* **2000**, *12*, 971−974.
(35) Tian, Y.; Akiyama, E.; Nagase, Y. *J. Mater. Chem.* **2003**, *13*, 1253−1258.
(36) Lee, J.; Lee, J.-I.; Sung, S.-J.; Chu, H. Y.; Park, J.-K.; Shim, H.-K. *Macromol. Chem. Phys.* **2004**, *205*, 2245−2251.
(37) Aldred, M. P.; Contoret, A. E. A.; Farrar, S. R.; Kelly, S. M.; Mathieson, D.; O'Neill, M.; Tsoi, W. C.; Vlachos, P. *Adv. Mater.* **2005**, *17*, 1368−1372.
(38) Kim, C.; Trajkovska, A.; Wallace, J. U.; Chen, S. H. *Macromolecules* **2006**, *39*, 3817−3823.
(39) Trajkovska, A.; Kim, C.; Marshall, K. L.; Mourey, T. H.; Chen, S. H. *Macromolecules* **2006**, *39*, 6983−6989.
(40) Geng, Y.; Culligan, S. W.; Trajkovska, A.; Wallace, J. U.; Chen, S. H. *Chem. Mater.* **2003**, *15*, 542−549.
(41) Yu, X.; Scheller, D.; Rademacher, O.; Wolff, T. *J. Org. Chem.* **2003**, *68*, 7386−7399.

MA702080Z